Published in final edited form as:
Neuroimage. 2013 December ; 83: . doi:10.1016/j.neuroimage.2013.06.066.

Ferumoxytol Enhanced resting state fMRI and Relative Cerebral Blood Volume mapping in Normal Human Brain

Helen D'Arceuil[1], **Alexandre Coimbra**[2], **Pamela Triano**[3], **Margaret Dougherty**[3], **Julie Melo**[3], **Michael Moseley**[1], **Gary Glover**[1], **Maarten Lansberg**[4], and **Francis Blankenberg**[5]

[1]Dept. of Radiology, Stanford University, CA, USA.

[2]Early Clinical Development, Genentech Inc., CA, USA.

[3]Department of Rehabilitation Services, Stanford University, CA, USA.

[4]Dept. Neurology, Stanford University, CA, USA.

[5]Pediatric Radiology, Stanford University, CA, USA.

Abstract

The brain demonstrates spontaneous low-frequency (< 0.1 Hz) cerebral blood flow (CBF) fluctuations, measurable by resting-state functional MRI (rs-fMRI). Ultra small superparamagnetic iron oxide particles have been shown to enhance task-based fMRI signals (cerebral blood volume fMRI or CBV-fMRI), compared to the BOLD effect, by a factor of ≈ 2.5 at 3T in primates and humans. We evaluated the use of ferumoxytol for steady state,resting state FMRI (CBV-rs-fMRI) and relative cerebral blood volume (rCBV) mapping, at 3 Tesla, in healthy volunteers. All standard resting state networks (RSNs) were identified in all subjects.On average the RSN Z-statistics(Melodic independent components)and volumes of the Visual and default mode (DMN)networks were comparable rCBV values were averaged forthe visual (Vis) and DMN networks and correlated with the corresponding DMN and Visual network Z statistics. There was a negative correlation between the rCBV and the Z-statisticsforthe DMN, for both BOLD and CBVrs-fMRI contrast (R^2= 0.63, 0.76).A similar correlation was not found for the visual network. Short repetition time rs-fMRI data were Fourier transformed to evaluate the effect of ferumoxytol on cardiac and respiratory fluctuations in the brain rs-BOLD, CBV signals. Cardiac and respiratory fluctuations decreased to baseline within large vessels post ferumoxytol.Robust rs-fMRI and CBV mapping is possible in normal human brain.

Introduction

We aimed to determine whether robust resting state functional magnetic resonance imaging (rs-fMRI) and cerebral blood volume (CBV) measures could be obtained from normal human brain after an intravenous infusion of a single dose of ferumoxytol. In addition, we investigated how the low level cardiac and respiratory contributions to the rs-fMRI signals would be affected by the presence of ferumoxytol. We also investigated whether higher resolution (approximately 2.3 mm^3) rs-fMRI images,of comparable resolution to the CBV

Address correspondence to: Helen E. D'Arceuil, helend2@stanford.edu, Phone: 650 515 0806, Address: Stanford University, Department of Radiology, The Lucas Center for MR Spectroscopy and Imaging, Mail Code 5488, Route 8, Stanford, CA, 94305-5488.

images, could be acquired after ferumoxytol injection. High resolution rs-fMRI can ultimately be useful for investigating the mechanistic aspects of the fMRI signal or for examining a wide range of stroke lesions during post-stroke repair and remodeling.

Studies have shown that the task-based fMRI signal can be enhanced using an intravascular monocrystalline iron oxide nanoparticle (MION) contrast agent (CBV-fMRI) compared to the blood-oxygenation (BOLD) signal (Leite et al., 2002) Ferumoxytol (Feraheme™) is an ultrasmall superparamagnetic iron oxide that was approved by the FDA as an iron replacement therapy for use in patients with chronic kidney disease. Ferumoxytol has a half life of about 15 hours in humans and may be injected as a rapid bolus (ferumoxytol package insert). Mandeville et al.(Mandeville, 2012)has shown, in non-human primates, that Feraheme increased fMRI contrast to noise by a factor of 2.5 at an MRI field strength of 3 Tesla, higher gains were realized at 1.5 T. However, for shorter stimulus durations (~4s) Leite et al.(Leite et al., 2002) showed a smaller gain (~1.7) in fMRI contrast after MION injection in nonhuman primates.Ferumoxytol has been used in humans for more accurately mapping CBV in brain tumor patients (Dosa et al., 2011; Gahramanov et al., 2011a; Gahramanov et al., 2011b).Recently, two clinical studies have reported markedly increased contrast-to-noise ratio (~3 fold) in task-based CBV-fMRIusing ferumoxytol(Baumgartner et al., 2012; Qiu et al., 2012)compared to BOLD based fMRI. In our study we investigated the use of ferumoxytol with standard, clinically applicable pulse sequences for acquiring CBV-rs-fMRIand cerebral blood volume metrics in the brains of normal human volunteers.

Methods

Human subjects

All procedures were approved by our institutional IRB panel and volunteers gave informed, written consent. Subjects were screened, prior to admission to the study, for iron sensitivity or other contrast agent allergy or sensitivity. They were also asked whether they had a history of low blood pressure. Eight subjects were enrolled in the study and imaged at least once;3of these subjects had a repeat scan at least3 weeks after the first.Resting state and cerebral blood volume data from 6 subjects were grouped; 1 subject fell asleep before the contrast enhanced scansand there was an incidental finding of an inclusion within the right frontal bone of another subject which caused signal dropout in the frontal-temporal brain. These two subjects were excluded from the group analyses.Noninvasive blood pressure and heart rate were measured during all scansGeneral Electric (GE)"InVivo" physiological monitoring system, GE Milwaukee, USA). In addition, subjects were monitored using the scanner's plethysmograph and respiration band (pneumatic belt). During the resting state acquisitions, subjects were asked to focus on a point on the head coilin front of them and stay awake. We confirmed that subjects were awake by speaking to them before and after the fMRI scan. Bilateral plastic clamps were applied to the frontal-temporal head areaover foam pads and additional foam pads applied to the side and top of the head to help alleviate head motion. All subjects wore ear plugs. During each MRI exam, all subjects received an injection of ferumoxytol (fixed dose of 510mgFe, which is the FDA approved dose for therapeutic use) given as a bolus at 0.5ml/sec using an MRI compatible power injector.

MRI

All images were acquired on a 3T GE Discovery MR 750 HD scanner. Signal reception used an 8 channel GE receive only head coil. Except for the fMRI scans, all acquisitions used product GE pulse sequences. For the rs-fMRI we used a productgradient recalled echo-echo planar imaging (GRE-EPI) sequence that was modified to automatically record the subject's respiration and heart rate during these scans].The following imaging protocol was used:

1. 3D structural T1-wt scan (3D-SPGR)

2. Multi-echo gradient-recalled echo (T2* mapping)
3. Dual-echo fast spin-echo (T2 mapping)
4. Resting-state fMRI (multi-slice)
5. High-speed fMRI (4-slice)
6. Dynamic susceptibility contrast scan during a bolus injection of ferumoxytol
7. Repeat of 2–5
8. Higher resolution rs-fMRI

Sequence parameters for rs-fMRI were as follows:GRE-EPITR 2450 ms, TE 30 ms (precontrast),TE 20 ms (postcontrast, to maximize contrast to noise according to Mandeville et al (Mandeville, 2012) matrix 64×64, 40 slices, NEX 1, FOV 240, phases 120, slice thickness 2.9 mm, 0.5 mmgap, flip angle77deg. In addition, higher resolution rs-fMRI series were acquired post-Ferumoxytol with the following imaging parameters: TR 2450 ms, TE 20 ms, matrix 96×96, and either 2.9/0.5 or 2.0/0.3mm slice/gap, flip angle 77deg, Slices 40, NEX1 , FOV 240, phases 120.

Low level cardiac and respiratory induced signal fluctuations occurring within the brain were measured using a high-speed GRE-EPIacquisition pre and post-ferumoxytol infusion with the following parameters:TR 250ms, TE 30ms, matrix 64×64, flip angle 33 deg, Slices = 4, NEX =1 , FOV 240, phases 360, 4 (2.9 mm) thick slices, 25 mm gap.TE was reduced to 20 ms post ferumoxytol injection.

Dynamic susceptibility (DSC) weighted imaging used a spin-echo echo planar imaging (SE-EPI) imaging sequence to follow the slow bolus of ferumoxytol (1 min. total bolus duration), with the following imaging parameters; TR 3650 ms, TE 60 ms, flip angle 90°, matrix 128 × 96, slice thickness 2.9 mm, 0.5 mm gap, 40 slices. A spoiled gradient echo, multi-slice multi-echo sequence was used to acquire T2* weighted images of the entire brain. The following parameters were used: TR 2000ms, 8 echoes: 3.67–41.7 ms (5.4 ms increments), 90° flip, matrix 240 × 240, slice thickness 2.9 mm thick, 40 slices, 0.5mm gap, 1 average. T2 mapping was effected with a fast spin echo imaging sequence; TR 4525, TE 12.78/102.2, ETL 8, flip angle 90°, matrix 256^2, NEX 1, slice thickness 2.9 mm, 0.5 mm gap.

Data processing

Resting state fMRI—Resting state fMRI data were processed using FEAT (fMRI Expert Analysis Tool) Version 5.98 and MELODIC (Multivariate Exploratory Linear Optimized Decomposition into Independent Components), FMRIB's Software Library, www.fmrib.ox.ac.uk/fsl, Oxford, UK. rs-fMRI data were registered to a standard brain template (Montreal Neurological Institute (MNI) 2mm standard brain)using FLIRT (Jenkinson et al., 2002; Jenkinson and Smith, 2001).The following pre-processing steps were was applied to the data; brain extraction (BET),motion correction (MCFLIRT), spatial smoothing using a Gaussian kernel of FWHM 3mm; grand-mean intensity normalization of the entire 4D dataset by a single multiplicative factor; highpass temporal filtering(Gaussian-weighted least-squares straight line fitting, with sigma = 100.0s), removal of the first 5 volumes data (MELODIC) and ICA components generated. Subsequently, the components were examined and unwanted components with extreme power spectra, sudden jumps in intensity, motion and susceptibility artifacts due to air signal flagged for removal. De-noised(unwanted components removed) data were re-processed to yield Z score (Z statistic) maps for independent components (ICA maps). ICA Z statistic maps were then transformed into MNI-2mm standard space and the networks verified using the Harvard-Oxford Cortical

and Sub-cortical Atlases in FSL.Summary statistics were calculated for each network by thresholding at Z=2 and measuring the volume and mean of thresholdedZ voxels.

In addition to the ICA analysis described above, we also used a whole brain ROI correlation approach, according to Shirer et al. {Shirer, 2012 #210,to test the reproducibility of our MELODIC results. ThisROI correlation approachdemonstrated close agreement between BOLD and CBV-rs-fMRI connectivity patterns (data not shown), in agreement with the MELODIC based results.

In order to identify common spatial patterns within this population we performed a comparison of the rs-fMRI network components from multiple subjects using the "multi-session temporal concatenation" feature in MELODIC. All datasets (after MELODIC processing) were first temporally concatenated to produce a 4D dataset followed by dual regression analysis.

Amplitude of the rs-fMRI signal fluctuations—To evaluate the effect of ferumoxytol on the amplitude of the rs-fMRI signal fluctuations we calculated the voxelwise mean and standard deviation (SD) of the signal timecourse in the EPI data series. We calculated the average mean and SD in the visual RSN, using the template ROI of Beckmann et al, {Beckmann, 2005 #196} for each subject before and after ferumoxytol injection.

High speedresting state FMRI data—For each slice, pixel intensities were normalized by dividing by the mean signal intensity over the entire slice. The normalized images werethen Fourier transformed along the Z axis followed by a magnitude calculation of the data. Thereafter, regions of interest in the sagittal sinus, cerebral and cerebellar cortices (entire extent) and aqueduct were measured from the frequency spectra.

T2* fitting—T2* weighted DICOM images were converted to ANALYZE format using in-house conversion software. Multi-echo data were checked for head motion and then fitted,MRVision software (MRVision Co, Redwood City, CA)usinga nonlinear algorithm to a mono-exponential equation of the form $M = M0 \exp(-TE/T2) + C$ (where the constant term C was fixed for each dataset) and T2* maps generated.The pre and post contrast T2* images were then processed as follows. If necessary, the pre and post contrast T2* images were co-registered using FSL-FLIRT.R2* maps (1/T2*) were generated and transformed to MNI 2mm standard space. ΔR2* maps (R2*post contrast images were subtracted from R2* pre-contrast images)were generated. In addition, T2* was measured over whole cortical gray matter ROIs(6 slices sampled over the extent of the brain, excluding ventricles) as well as in the sagittal sinus (7 adjacent slices) before and after ferumoxytol injection.

CBV estimation—Parametric relative cerebral blood volume maps (rCBV) were calculated as follows: rCBV = ΔR2* / [blood iron concentration],(Barbier et al., 2001). Since the postcontrast T2* in blood (sagittal sinus) was very short and difficult to measure accurately (see below), empirical calculation of blood iron concentration was challenging. Therefore blood iron concentration for each subject was estimated according to the following expression:

[blood Fe, mM] = [injected Fe, mM]/ (total blood volume, L).

Individual subjects'total blood volumes (BV) were calculatedbased ongender, height and weightaccording to Nadler et al(Stenger et al., 2012)(Nadler et al., 1962)

(total BV, male) = $0.3669 * (\text{height, m})^3 + 0.03219 * (\text{weight, kg}) + 0.6041$.

(total BV, female) = $0.3561 * (\text{height, m})^3 + 0.03308 * (\text{weight, kg}) + 0.1833$.

The thresholded DMN and VIS RSNs were mapped onto the rCBVmaps and regional rCBV values corresponding to the regional resting state activation maps computed for each subject. Mean rCBV and Z-statistics were compared between BOLD and the corresponding CBV-rs-fMRI RSNs.

Results

Human Volunteers

All subjects tolerated the ferumoxytol infusion well; no adverse eventswere experienced on scan day or reported thereafter.Heart rate (HR) in beats per minute (BPM) and mean arterial blood pressure (MABP, mmHg) are reported in Table 1. Also reported here are HR and respiration values that were calculated from the high speed resting state EPI data. There is fairly good correspondence between the measured and calculated heart rate.

BOLD and ferumoxytol enhanced (CBV) Resting State Networks

BOLD and CBV resting state networks (RSNs) were identified in all subjects.Figure 1(A) showsaverage group z statistics (thresholded at Zmin = 2.0) and compared with standard RSN (also thresholded at Z min= 2.0) for sevenwell established RSNs for paired BOLD and ferumoxytol data from 6 subjects.All components are maximally scaled according to the Z statistic scale shown.The 8^{th} RSN, the executive control (also in Figure 1 (A), was only seenin the BOLD dataset. These data were generated from images with the same voxel resolution ($3.75 \times 3.75 \times 3.4$ mm^3, hereafter referred to as RES-0).The mean Z statistics and corresponding volume of the default mode and visual RSNs for the individual subjects are plotted in Figure 2. There is good agreement between the visual extent of the RSNs from BOLD and CBV rs-fMRI, as well as the mean Z statistics and network volume.Averaged data showing the mean (thresholded minimum = 2) default mode network (DMN) and visual (VIS) networks Z statistics for the subjects (n=6, 1timepoint) are presented in Table 2.

Additional coherent resting state patterns (Z min = 0) were also identified from both the BOLD and ferumoxytoldatasets, Figure 1 (B). A frontal cortex RSN pattern involving the following frontal cortical regions, the frontal-medial, frontal orbital, frontal pole and sub-callosal cortices, was identified, Figure 1 (B). This patterns is consistent with the frontal network reported by Stenger et al (Stenger et al., 2012)and it is hypothesized to belong to the DMN. Also, three more resting state patterns (1, 2, 3) were identified from the ferumoxytol data only; (1) Bilateral resting state pattern involving the pre and post central, supramarginal (anterior and posterior division), angular gyri, the superior lateral occipital cortex and the superior parietal lobule, possibly the DPN2 network, (2) A resting state pattern involving the precuneous and cuneal cortex, the lateral occipital cortex and the temporal occipital fusiform gyrus and (3) A resting state pattern (consistent with regions that compose the temporal-occipital pathway (ventral stream), described by Damoiseaux et al (Damoiseaux et al., 2008).

In addition, higher resolution ferumoxytol enhanced rs-fMRI data were acquired at the following voxel dimensions;($2.5 \times 2.5 \times 3.4mm^3$) hereafterreferred to as RES-1 and ($2.5 \times 2.5 \times 2.3$ mm^3) hereafter referred to as RES-2. Figure 3 shows examples of the visual network (one subject) overlaid on their respective echo planar images. The EPI images clearly show low signal in the larger vessels within the brain. The higher resolution ferumoxytol enhanced images (RES 1, 2) show clearer delineation of the RSNs with respect to the nearby blood vessels when compared to the RES-0 images. BOLD RES −1 data were also acquired in one brain, shown in Figure 3. The high resolution BOLD data shows much less sensitivity, compared to its ferumoxytol enhanced counterpart, data for detecting the visual RSN.

Amplitude of fMRI Signal Fluctuations

Inspection of the scanner transmit and receive gain settings for the rs-fMRI series showed no significant changes pre- and post-ferumoxytol injection, suggesting that it is reasonable to compare the changes in signal intensity. Across the group, the mean signal intensity in the template visual RSN decreased by a factor of 0.57 ± 0.12 after ferumoxytol injection, however the mean standard deviation of the signal increased by a factor of 2.2 ± 1.1.

Cardiac and Respiratory Signal Fluctuations within the Brain

Low level cardiac and respiratory fluctuations were within the 0–1.0 Hz range, respiratory at about 0.2 Hz (0.2 ± 0.1) and cardiac at about 0.9 Hz (1.0± 0.2). Figure 4(A, B) show spectra (top) of regional cardiac and respiratory fluctuations, pre and post-feruxomytol, within the sagittal sinus and cerebral cortex of one subject.The cerebellar cortex showed a similar pattern to that of the cerebral cortex, data not shown. As expected, all signal within the sagittal sinus rapidly decays into the noise floor after ferumoxytol administration.However, within the cerebral cortex these fluctuations varied individually. Cardiac fluctuations generally showed slight increases from baseline with two exceptions, one subject showed a relatively large increase while another decreased. Respiratory fluctuations were generally slightly decreased post ferumoxytol although two subjects showed increased fluctuations. Gradient echo images (bottom), along with their respective cardiac and respiratory spectral components (top), pre and post ferumoxytol are shown in Figure 4, Aand Brespectively.The cardiac and respiratory fluctuations measured in individual subjects are presented in Figure 5 (C, D).

Brain T2* and rCBV Mapping

Cortical gray matter T2* decreased from 51.5 ± 3.3 ms to 29.9 ± 3.1 ms after ferumoxytol infusion. Table 3 shows eachsubjects' individual relaxation time changes in the cortex and blood pool, as well as bodyweight, injected iron dose (mg/Kg) and the estimated millimolar blood iron concentration (used in rCBV calculation).Mean ΔR2* in the cortex was 0.027 ± 0.005 ms^{-1}, compared to 0.45 ± 0.13 ms^{-1} in blood. While T2* measurement in the cortex was quite accurate (Figure 6), the signal in the sagittal sinus post-contrast decreased close to the noise level by the second echo, rendering T2* measurement inaccurate. As a result, *measured* blood ΔR2* was very weakly and inversely correlated with the *estimated* blood ion concentration (R^2 = 0.09) as well as the measuredcortical ΔR2* (R2 = 0.14). In contrast, cortical ΔR2* was positivelycorrelated with the estimated blood iron concentration (R^2 = 0.59), as expected.

Z score and rCBV Mapping

Relative cerebral blood volume maps of the normal human brain showed lower CBV within the white matter compared to the cortex, Figure 5 (F), as expected. CBV values in activated regions corresponding to the DMN and visual networks are given in Table 2 above. Figure 6 (A-D) shows the relationship between mean Z statistic and rCBV in the network volume (thesholded at Z=2) for DMN and Visual RSNs. There appears to be a trend ofdecreasing rCBV with increasing Z-statistic for both BOLD and CBV-rs-fMRI data in the default mode network but the opposite effect in seen in the visual network, at least for BOLD contrast.

Discussion

In this study, all subjects tolerated the study procedures very well.We did not observe any adverse events with the use of the ferumoxytol contrast agent,even though there are known adverse events including hypotension and anaphylaxis, as detailed in the Feraheme product insert, associated with its use.

We found that ferumoxytol enhanced CBV-rs-fMRI is robust and shows the expected major networks, very similar to those seen by means of the BOLD effect at 3T. Group analysis of the rs-fMRI and CBV-rs-fMRI data revealed 7 common networks in each category. The executive control network was not identified in the CBV-rs-fMRI data, only from the BOLD data. In contrast, 3 additional CBV-rs-fMRI RSNs were identified, shown in Figure 1B, one RSN that may be the DPN2 and another network that is consistent with the ventral stream (Damoiseaux et al., 2008).The third network remains uncharacterized.

Increased cardiac and respiratory (some individuals) signals post ferumoxytol suggests that correcting for these effects may be more important with CBV-rs-fMRI. However, in the individuals with increased cardiac and/or respiratory fluctuations, robust resting state networks were still clearly identified. While correcting for these slight increases should only enhance the strength of these networks,as has been published previously (Birn et al., 2008; Chang and Glover, 2009), in our data there was no clear relationship between changes in the cardiac/respiratory fluctuations post-ferumoxytol and the measured RSNs. For example, in a subject that had no measureable low level respiration fluctuations within the cortex post ferumoxytol(low level cardiac and respiratory fluctuations decreased compared to the respective BOLD derived values. In contrast, in another subject that showed increased respiration fluctuation post ferumoxytol, the DMN volume increased while the visual network volume decreased. It may simply be that any amplification of cardiac signal fluctuations following ferumoxytol injection is too subtle to impact the detection of RSNs using MELODIC.

Previously published data have shown that ferumoxytol enhanced *task-based* fMRI results in a 3 fold increase in contrast-to-noise in the brain of nonhuman primates (using 16–32s stimuli)(Mandeville, 2012)and a 2–3 fold increase in humans at 3T (15–50s stimuli) (Baumgartner et al., 2012; Qiu et al., 2012)after a 510mg injection of the agent. On the other hand,Liete et al(Leite et al., 2002) performed task based resting state experiments in nonhuman primates using an 8–10mg/kg injection of aMION agent at 3T and showed only a 1.7 fold contrast increase compared to BOLD for a short4s stimulus and26s stimulus interval (compared to a 3 fold increase for a 60s stimulus) .While that nonhuman primate study used a different contrast agent the iron dose was very similar to that used in our and previous human CBV-fMRI studies. For the case of resting state fMRI,most of the energy contributing to the measured RSNs is in the 0.0–10.1 Hz range, i.e. periods of 10–100s. This could be interpreted as a response to a stimulus of 5–50s with 5–50s rests (assuming 1:2 duty cycles). In fact for the RSNs we detected, most of the power spectra peaked around 0.04Hz or less (25s or longer period) suggesting that by comparison to the task-based CBV-fMRI data discussed above, our experiments are somewhere in the middle of the range in terms of 'stimulus duration'. In our study, we detected about a 2 fold increase in SD of the fMRI signal in the visual area after ferumoxytol injection. This did not translate into a similar increase in Z-statistic for the visual RSN however. In fact we observed close agreement in both volume and mean Z-statistics of the major RSN metrics for BOLD and CBV-rs-fMRI at 3T. Given the complexities of the ICA analysis, one may not expect a linear relationship between Z-statistic and signal fluctuation amplitude. In addition, the observed increase in cardiac induced CBV-fMRI signal fluctuations may play a role.

There are additional considerations that may affect the relative size and strength of CBV and BOLD derived RSNs. These volunteer data involved extended scan time in most individuals and may reflect the subject's varying compliance (wakefulness, active thinking) with increasing study time (the CBV scan was always later than the BOLD scan).There are clearly differences in resting blood flow states among different individuals, this has been previously published by Ito et al (Ito et al., 2001)although, as seen in Table 2, the DMN at least was very consistent across our group of subjects. Also, as can be seen in Table 1, some

subjects showed greater variation in resting heart and respiration ratesduring the acquisition and study period.However, a more likely explanation may be a difference in underlying contrast mechanisms for task-based and resting state signals. Resting state signals are in general smaller than in task based experiments and may be more dependent on changes in CBF relative to changes in CBV(i.e. there is a nonlinear relationship between CBV and CBF changes during activation (Buxton et al., 2004)whether spontaneous (resting state) or task based. As such, enhancing the blood pool in the resting state regimen may be less advantageous.

Signal within the larger vessels of the brain decreased to the level of the background noise after ferumoxytol injection and this allowed better visualization of the cerebral cortex and white matter. Both of these features improved the quality of the higher voxel resolution CBV-rs-fMRI scans which showed a clear advantage for visualization and delineation of the RSNs with respect to the vasculature. We observed that higher resolution CBV-rs-fMRI yielded well defined RSNs whereas the comparable BOLD RSN appeared more fragmented.In the case of post-stroke neurological impairment that can affect any aspect of the brain function, e.g., motor, visual and or speech, the ability to more accurately and reliably map the peri-lesional tissue will offer a way to non-invasively monitor functional changes around and distant to the lesion as the body rehabilitatesand the brain re-organizes accordingly.In this study we have investigated an approximately 70% increase in voxel resolution with the ferumoxytol enhanced rs-fMRI images in reasonable time (approximately 5 mins). Further improvements in spatial resolution (smaller voxels) should be achievable by using a 32 channel receive coils, for example.

The chronic stroke period offers a greatly extended time window for therapies aimed at promoting brain plasticity and or remodeling. Robust, clinically appropriate MRI neuroimaging sequences that can serially and noninvasively evaluate microstructural and functional aspects of the brains of the post-stroke patient is important for monitoring brain plasticity, remodeling and therapeutic interventions. The ability to also map regional CBV on a pixel by pixel basis at higher resolution (equivalent to that of the rs-FMRI scans) thanis currently attainable with DSC gadolinium DTPA bolus tracking, will facilitate the assessment and monitoring of angiogenesis (sprouting of new capillaries from pre-existing vessels) withinand around the peri-lesional tissue in the post stroke brain, in the early (within 3 weeks) in stroke recovery period. These newly formed vessels can then be monitored as they increase in size, as well as theirprogressive maturation into mature vascular networks(Hayashi et al., 2003). This technique may also prove useful for monitoring therapies aimed at increasing perfusion within the brain, especially after stroke.Vasoactive drugs, such as Sildenafil, have been tested in preclinical models of stroke and have been shown to enhance blood flow and angiogenesis in the ischemic border-zone(Ding et al., 2011). In addition, Sidenafil has been shown to be safe in a small study of patients with mild to moderate stroke(Silver et al., 2009). In addition, there is currently an ongoing clinical trial aimed at establishing the efficacy of sildenafil for sub-acute ischemic stroke treatment (http://clinicaltrials.gov/show/NCT00452582).

The administration of a single dose of ferumoxytol allows us to measure both cerebral blood volume enhanced rs-fMRI and relative CBV during the same scan period. We observed a negative correlation between mean rCBV and DMN Z-statistic, measured in the same tissue volume, however the significance of this finding is unclear and warrants further investigation in a larger number of subjects. Nevertheless,higher resolution CBV-rs-fMRI and rCBV scans will facilitate easier and more accurate data co-registration and regional mapping within the brain, as reported here, and may also find application in other areas of study as suggested below.

Several studies have sought to understand the effects that anesthetic and analgesic agents and other drugs have on the brain and, in particular, how the fMRI derived resting state and task activated networks are affected. For example, it has been reported that anesthesiaalters the cerebral blood flow (CBF)- blood oxygen level dependent (BOLD) coupling(Stamatakis et al., 2010). However, BOLD contrast is also dependent on CBV. In future, BOLD and CBV activated networks along with cerebral blood volume metrics (in the same subject) using ferumoxytolmay prove useful to decipher CBV and CBF decoupling during neuronal and vascular challenges. Ferumoxytol enhancement may also be useful in characterizingchanges in the activated brain networks and their attending cerebral blood volume in the presence of novel pharmacological agents i.e., used as a tool in drug development. In this context. studies can easily be performed in animals and, where appropriate, nonhuman primates as a prequel to studies in awake or anesthetized humans.

In summary, we have shown that feruxomytol allows the acquisition of high resolution rs-fMRI and CBV measures in the brain within a single scan session, without the need for specialized pulse sequences. Increased contrast to noise may allow more accurate regional mapping of relative CBV and resting state networks.

Acknowledgments

This work was supported by grants from the following National Institutes of Health (NINDS-NS47607 (MM/HD) and (NIBIB-5P41EB015891-19 (GG). I would also like to thank Kevin Epperson, Carla Epperson, Anne Sawyer and Lanzie Rivera.

References

Barbier EL, Lamalle L, Decorps M. Methodology of brain perfusion imaging. J Magn Reson Imaging. 2001; 13:496–520. [PubMed: 11276094]

Baumgartner, R.; Cho, W.; Coimbra, A.; Gargano, C.; Iannone, R.; Struyk, A.; Fox, R.; Wang, Z.; Zhao, F.; Williams, D.; Reese, T.; Henry, B.; Petersen, E.; Chen, C.; Feng, D.; Apreleva, S.; Evelhoch, J. Evaluation of a functional MRI Assay Using a Novel USPIO Contrast Agent (Ferumoxytol) in Normal Healthy Volunteers. Melbourne, Australia: International Society for Magnetic Resonance in Medine; 2012. p. 2885

Birn RM, Murphy K, Bandettini PA. The effect of respiration variations on independent component analysis results of resting state functional connectivity. Hum Brain Mapp. 2008; 29:740–750. [PubMed: 18438886]

Buxton RB, Uludag K, Dubowitz DJ, Liu TT. Modeling the hemodynamic response to brain activation. Neuroimage. 2004; 23(Suppl 1):S220–S233. [PubMed: 15501093]

Chang C, Glover GH. Effects of model-based physiological noise correction on default mode network anti-correlations and correlations. Neuroimage. 2009; 47:1448–1459. [PubMed: 19446646]

Damoiseaux JS, Beckmann CF, Arigita EJ, Barkhof F, Scheltens P, Stam CJ, Smith SM, Rombouts SA. Reduced resting-state brain activity in the "default network" in normal aging. Cereb Cortex. 2008; 18:1856–1864. [PubMed: 18063564]

Ding G, Jiang Q, Li L, Zhang L, Zhang Z, Lu M, Li Q, Gu S, Ewing J, Chopp M. Longitudinal magnetic resonance imaging of sildenafil treatment of embolic stroke in aged rats. Stroke. 2011; 42:3537–3541. [PubMed: 21903952]

Dosa E, Tuladhar S, Muldoon LL, Hamilton BE, Rooney WD, Neuwelt EA. MRI using ferumoxytol improves the visualization of central nervous system vascular malformations. Stroke. 2011; 42:1581–1588. [PubMed: 21493906]

Gahramanov S, Muldoon LL, Li X, Neuwelt EA. Improved perfusion MR imaging assessment of intracerebral tumor blood volume and antiangiogenic therapy efficacy in a rat model with ferumoxytol. Radiology. 2011a; 261:796–804. [PubMed: 21940504]

Gahramanov S, Raslan AM, Muldoon LL, Hamilton BE, Rooney WD, Varallyay CG, Njus JM, Haluska M, Neuwelt EA. Potential for differentiation of pseudoprogression from true tumor

progression with dynamic susceptibility-weighted contrast-enhanced magnetic resonance imaging using ferumoxytol vs. gadoteridol: a pilot study. Int J Radiat Oncol Biol Phys. 2011b; 79:514–523. [PubMed: 20395065]

Hayashi T, Noshita N, Sugawara T, Chan PH. Temporal profile of angiogenesis and expression of related genes in the brain after ischemia. J Cereb Blood Flow Metab. 2003; 23:166–180. [PubMed: 12571448]

Ito H, Takahashi K, Hatazawa J, Kim SG, Kanno I. Changes in human regional cerebral blood flow and cerebral blood volume during visual stimulation measured by positron emission tomography. J Cereb Blood Flow Metab. 2001; 21:608–612. [PubMed: 11333371]

Jenkinson M, Bannister P, Brady M, Smith S. Improved optimization for the robust and accurate linear registration and motion correction of brain images. Neuroimage. 2002; 17:825–841. [PubMed: 12377157]

Jenkinson M, Smith S. A global optimisation method for robust affine registration of brain images. Med Image Anal. 2001; 5:143–156. [PubMed: 11516708]

Leite FP, Tsao D, Vanduffel W, Fize D, Sasaki Y, Wald LL, Dale AM, Kwong KK, Orban GA, Rosen BR, Tootell RB, Mandeville JB. Repeated fMRI using iron oxide contrast agent in awake, behaving macaques at 3 Tesla. Neuroimage. 2002; 16:283–294. [PubMed: 12030817]

Mandeville JB. IRON fMRI measurements of CBV and implications for BOLD signal. Neuroimage. 2012; 62:1000–1008. [PubMed: 22281669]

Nadler SB, Hidalgo JH, Bloch T. Prediction of blood volume in normal human adults. Surgery. 1962; 51:224–232. [PubMed: 21936146]

Qiu D, Zaharchuk G, Christen T, Ni WW, Moseley ME. Contrast-enhanced functional blood volume imaging (CE-fBVI): enhanced sensitivity for brain activation in humans using the ultrasmall superparamagnetic iron oxide agent ferumoxytol. Neuroimage. 2012; 62:1726–1731. [PubMed: 22584230]

Silver B, McCarthy S, Lu M, Mitsias P, Russman AN, Katramados A, Morris DC, Lewandowski CA, Chopp M. Sildenafil treatment of subacute ischemic stroke: a safety study at 25-mg daily for 2 weeks. J Stroke Cerebrovasc Dis. 2009; 18:381–383. [PubMed: 19717023]

Stamatakis EA, Adapa RM, Absalom AR, Menon DK. Changes in resting neural connectivity during propofol sedation. PLoS One. 2010; 5:e14224. [PubMed: 21151992]

Stenger VA, Poser B, Deng W, Anderson R. Susceptibility Artifacts in Resting State BOLD fMRI. OHBM. 2012:#625.

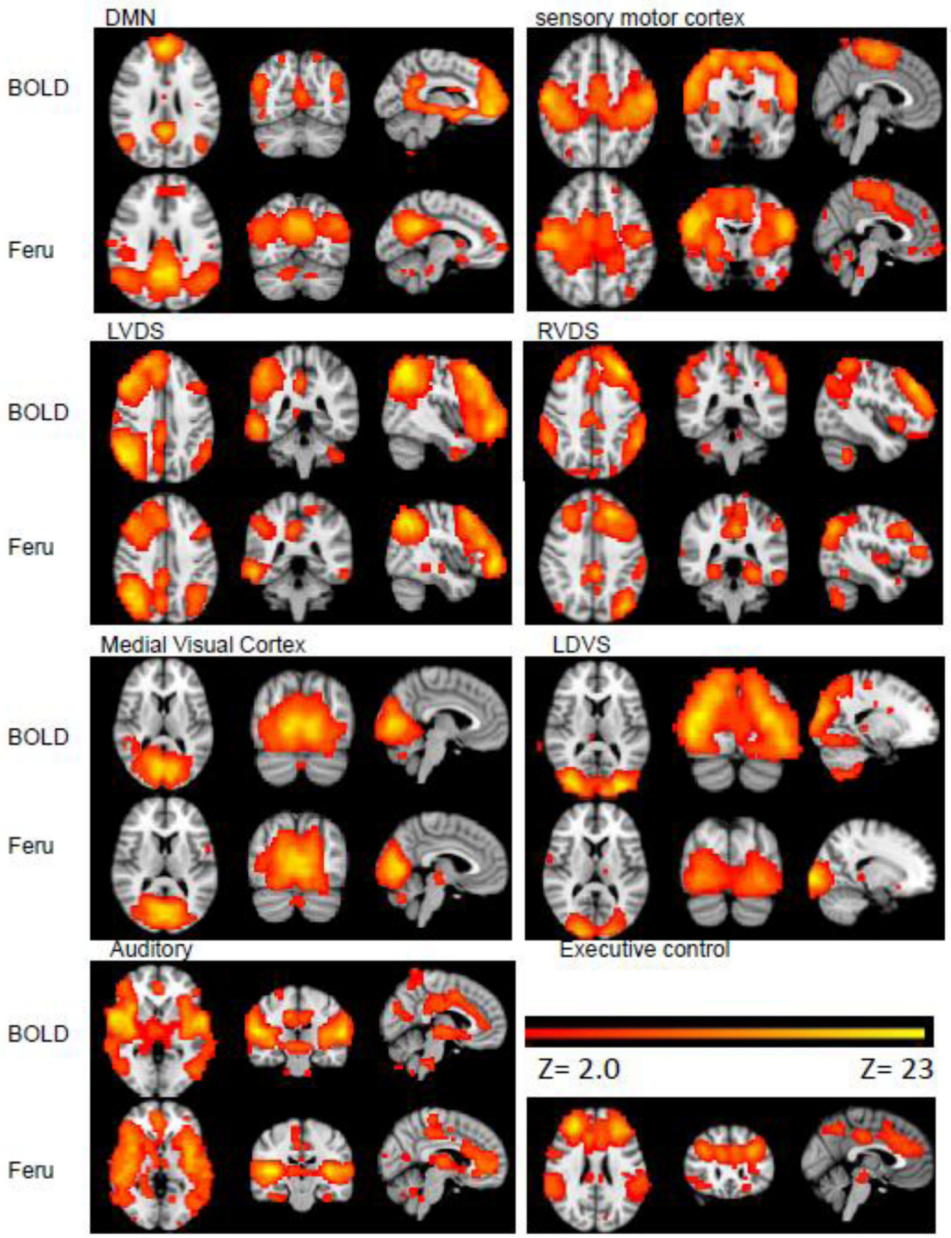

a

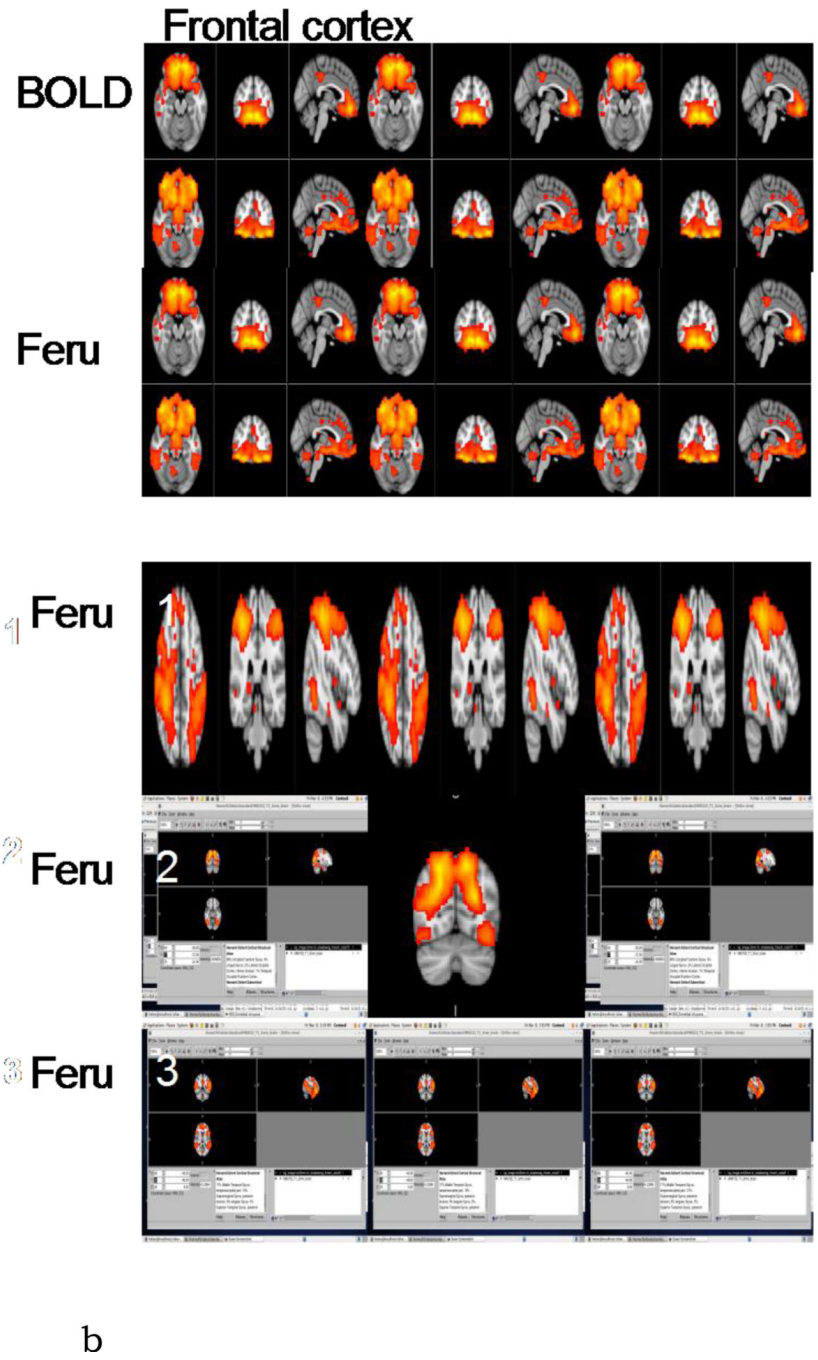

Figure 1.

(A): BOLD and ferumoxytol (Feru) enhanced (Res 0) RSNs overlaid on the standard T1 2mm MNI brain; default mode network (DMN), lateral and medial visual cortex, sensory motor (SMN), left and right dorsal visual stream (LDVS and RDVS),) and auditory (AUDIT) networks. The executive network was only identified from the Feru data. These networks show good correspondence with each other and the standard RSN templates of Beckmann et al [28]. Networks thresholded at Z min = 2 and confirmed with the standard RSNs.All RSNs were displayed according to the Z stat scale shown here.

B: Additional coherent resting state patterns were identified from both the BOLD and Feraheme datasets. The frontal cortex is consistent with the frontal network reported by

Stenger et al (Stenger et al., 2012) and it is hypothesized to belong to the DMN. Also, three more resting state patterns (1, 2, 3) were identified from the ferumoxytol data only; (1) Bilateral resting state pattern involving the pre and post central, supramarginal (anterior and posterior division), angular gyri, the superior laterial occipital cortex and the superior parietal lobule, possibly the dorsal pathway network (DPN2) temporal-parietal aspect. (2) A resting state pattern involving the precuneous and cuneal cortex, the lateral occipital cortex and the temporal occipital fusiform gyrus and (3) A resting state pattern (consistent with regions that compose the temporooccipital pathway (ventral stream), described by Damoiseaux et al (Damoiseaux et al., 2008).

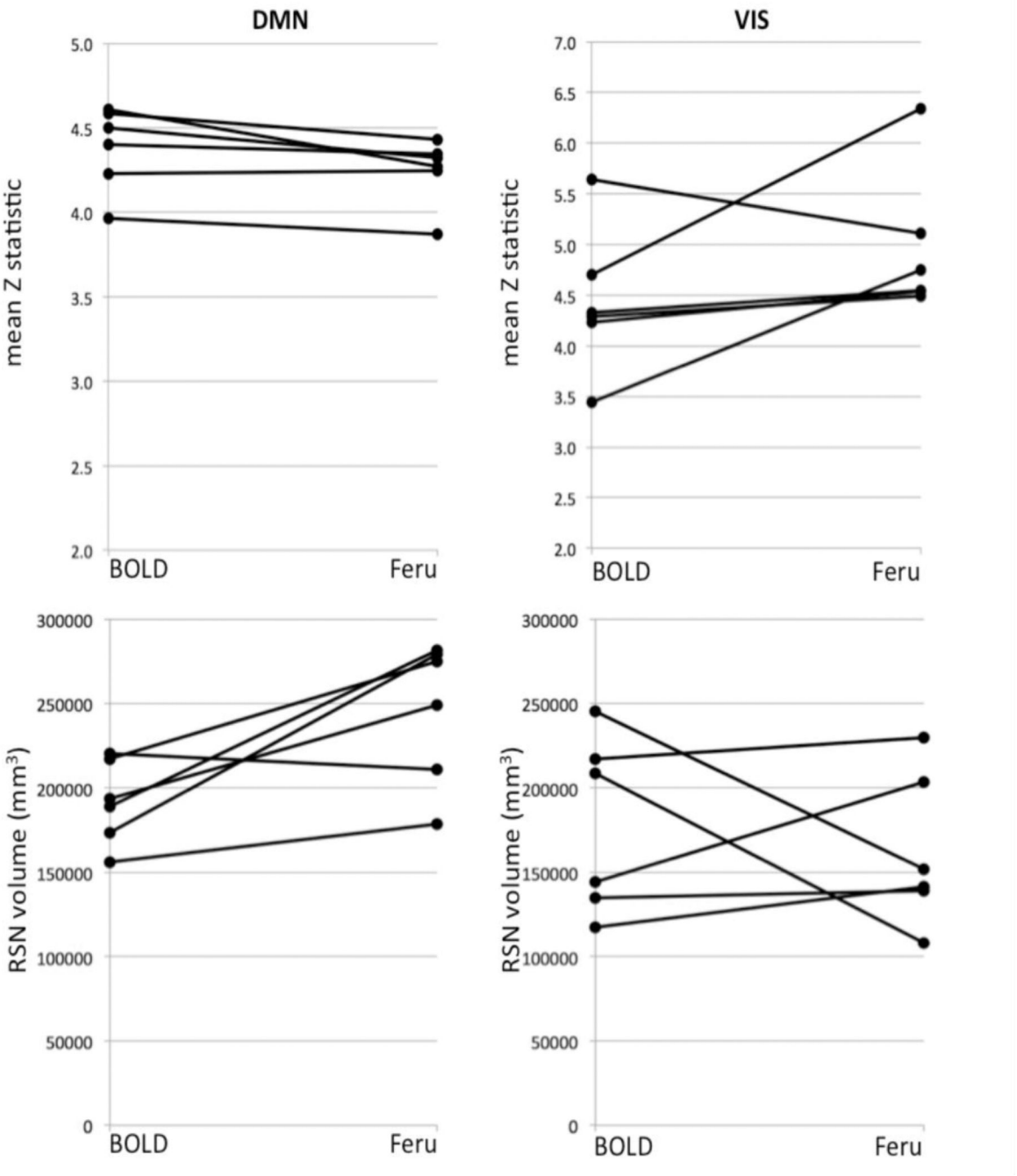

Figure 2.
Individual changes in mean Z statistic (top, minimum threshold of 2) and corresponding RSN volume (bottom) in default mode (left) and visual (right) RSNs from rs-fMRI scans before (BOLD) and after (Feru) ferumoxytol injection.

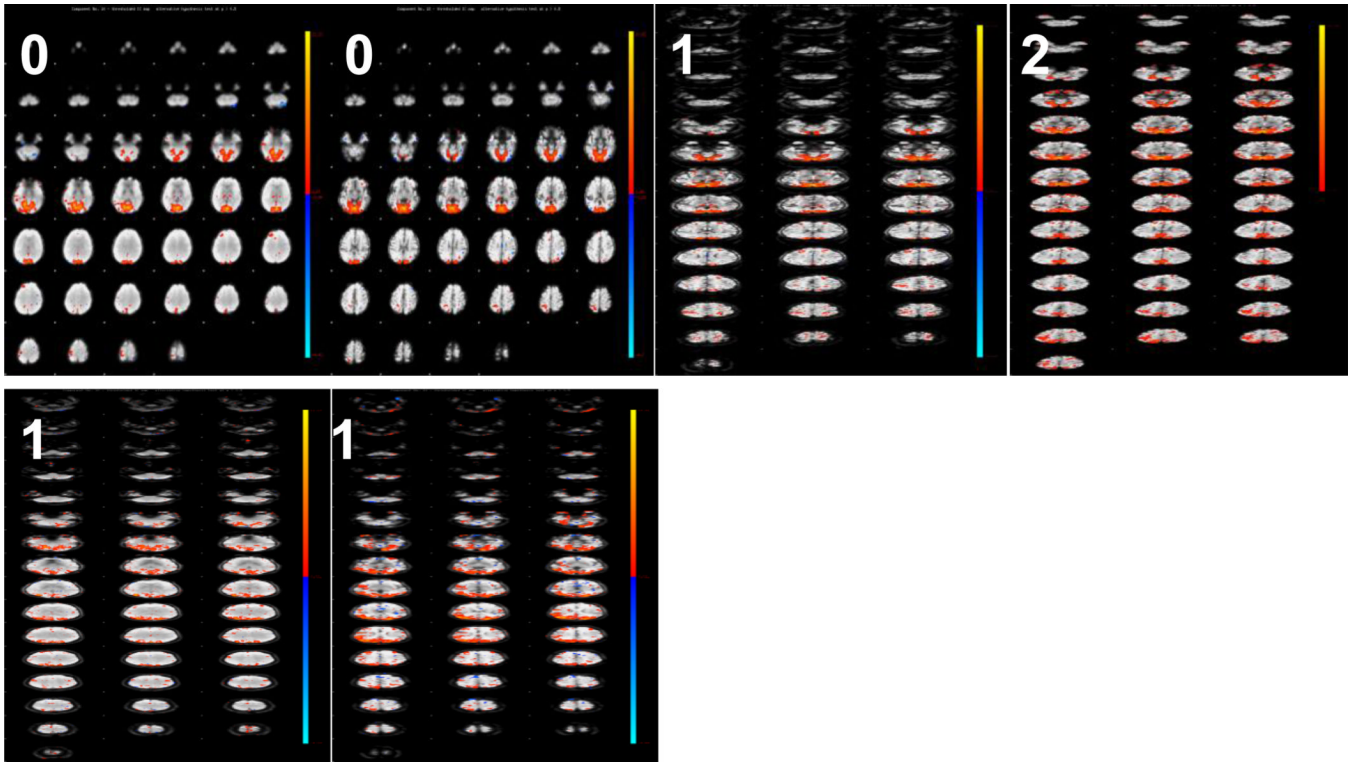

Figure 3.
Comparison of BOLD and CBV-rs-fMRI spatial resolution. Left-right: RES-0 BOLD and CBV, RES-1 CBV, RES-2 CBV for Visual RSNs for one subject. The high resolution ferumoxytol enhanced images allow much better delineation of the resting state networks in relation to the anatomy and vascular elements. In comparison (bottom row) the high resolution BOLD visual network is much smaller than the ferumoxytol enhanced visual network (another volunteer).

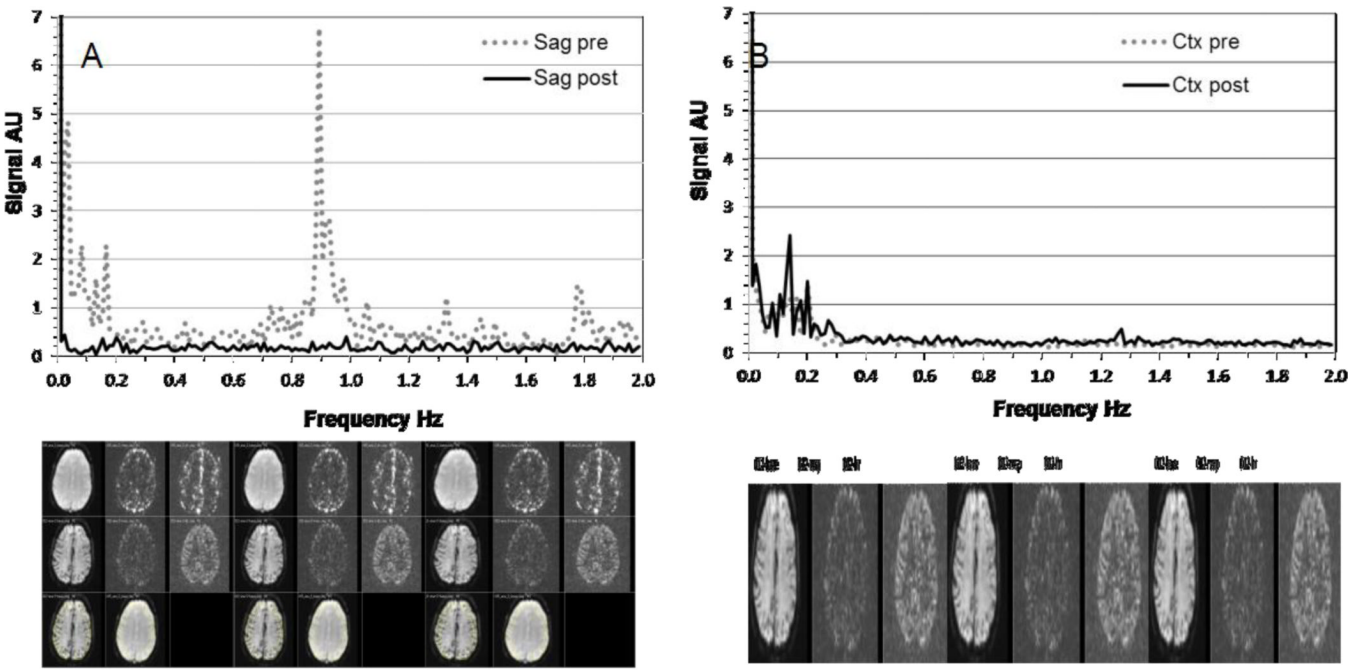

a-b

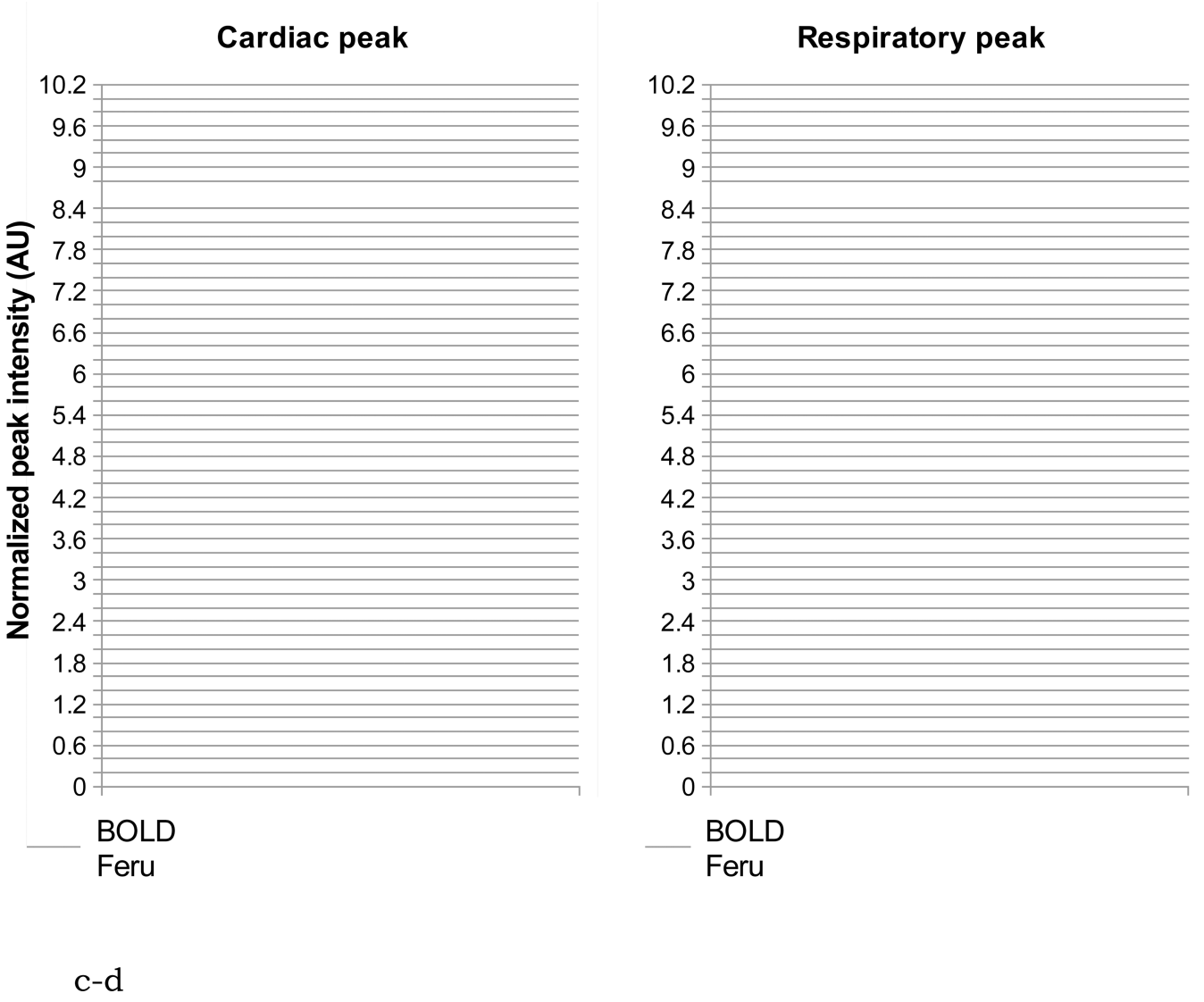

Figure 4.

(A, B): Frequency spectra (top) showing cardiac and respiratory fluctuations during high speed resting state fMRI acquisitions, pre and post ferumoxytol in one subject. The respiratory peak is at 0.16 Hz while the cardiac peak is at 0.89 Hz, corresponding to respiration and cardiac rates of 10 breaths per minute and 54 beats per minute, respectively. Both cardiac and respiratory pulsations are decreased within the sagittal sinus post ferumoxytol infusion. In cortical gray matter however, respiratory pulsations decreased but cardiac fluctuations increased in this subject. Gradient echo images (bottom) pre (A) and post (B) ferumoxytol are shown below their respective spectra; baseline EPI (bottom), respiratory and cardiac images respectively.

(C, D): Individual cardiac (C) and respiratory (D) fluctuations measured in cortical gray matter from the high speed resting state scans before (0) and after (1) ferumoxytol injection. There is a marked trend to greater cardiac fluctuations post ferumoxytol and a weak trend to decreased respiratory fluctuations.

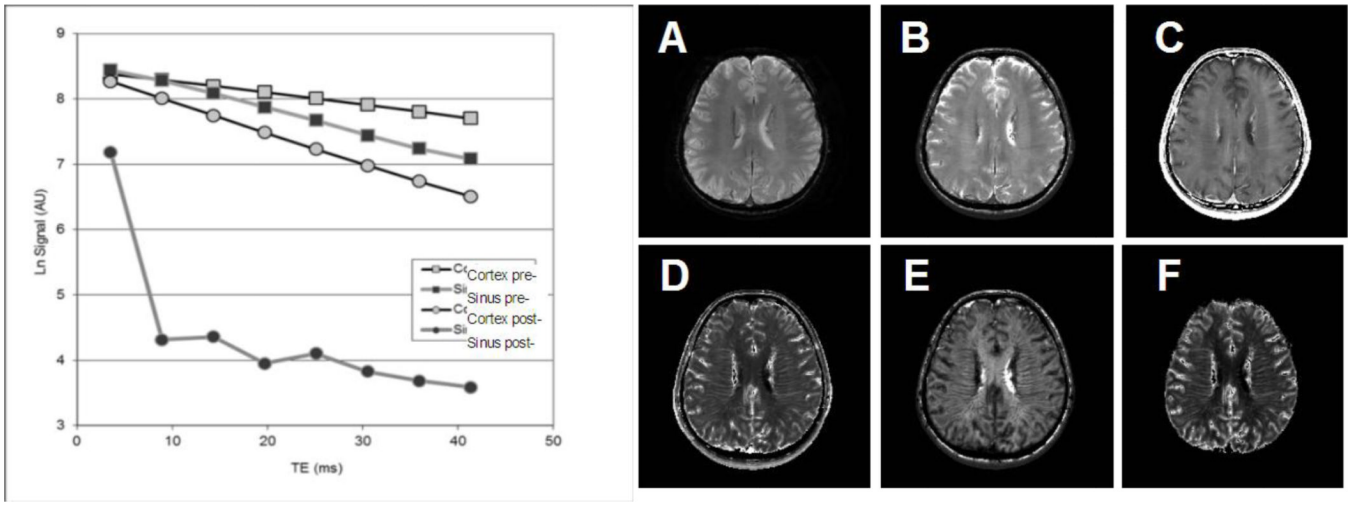

Figure 5.

Left: regional plots of the T2* decay curves within the cortex and sagittal sinus, pre- and post-ferumoxytol injection plots showing exponential T2* decay within the cortex (pre and post ferumoxytol) and the sagittal sinus (pre ferumoxytol). Right: T2* images and maps of the brain of one subject; (A) gradient echo image (TE-41.7 ms), (B) T2* map and (C) R2* map pre-ferumoxytol infusion, (D) T2* map and (E) R2* map post -ferumoxytol infusion. (F) ΔR2* map (R2* post – R2* pre, proportional to CBV).

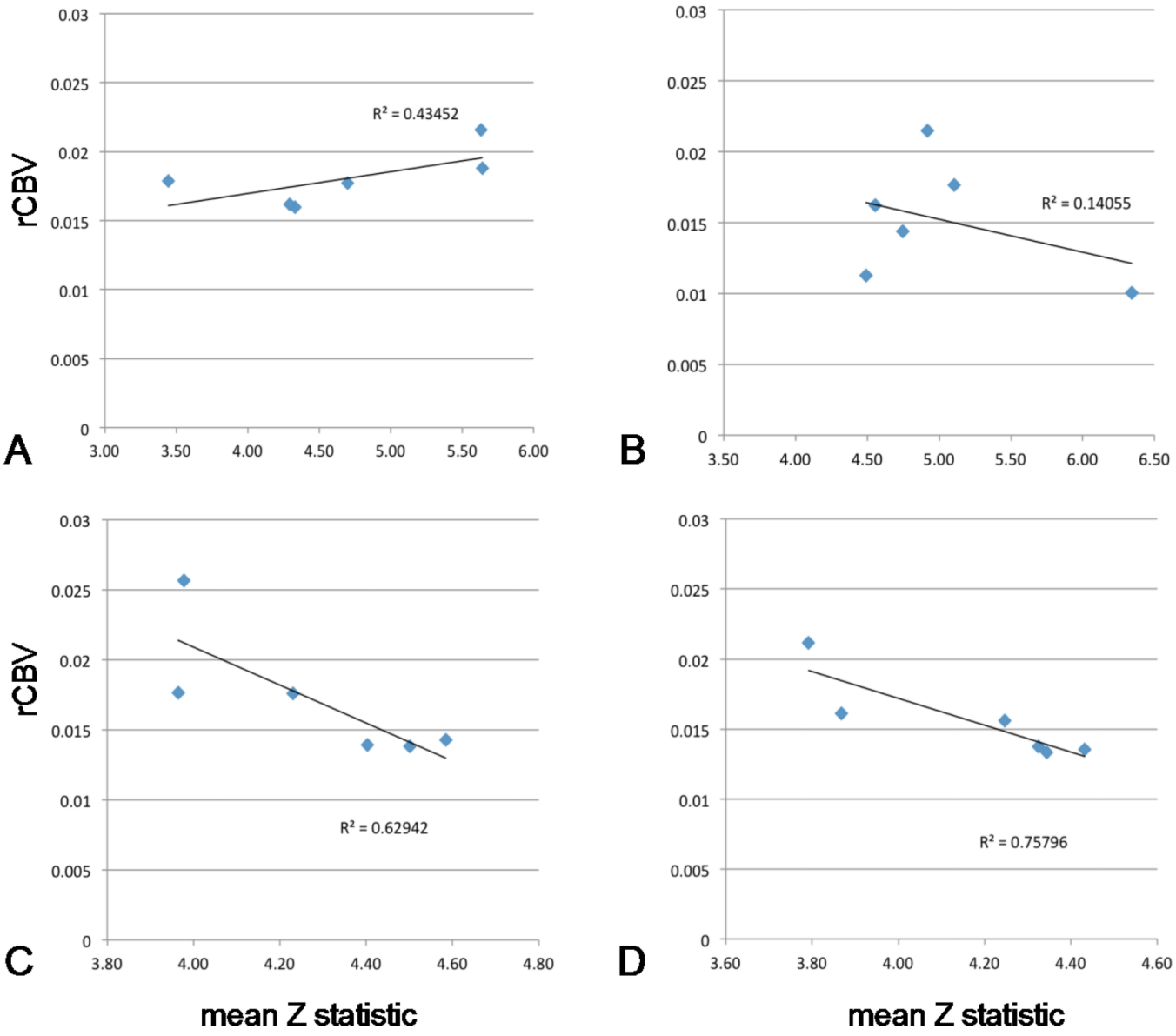

Figure 6.
(A–D): rCBV against mean Z statistic for Visual (A,B) and DMN (C,D) RSNs from BOLD (A,C) and CBV (B,D) rs-fMRI data. The DMN shows a more consistent trend for lower rCBV at higher Z statistic.

Table 1

Measured physiological parameters, HR (beats per minute) and non-invasive mean arterial blood pressure, MABP, for all subjects along with the calculated HR and respiration (breaths per minute) values. The latter were measured from the peaks in the frequency spectra that were derived from the high speed rs-fMRI data.

Subjects #	MABP (mmHg)	Heart Rate (HR)	HR (high speed rs-FMRI)	Respiration (high speed rs-fMRI)
1	88.3 ± 7.9	74.5 ± 5.3	-	-
1.1 (re-test)	79.0 ± 4.0	66.0 ± 7.0	54	10
2	88.3 ± 7.0	74.5 ± 5.3	72	16
2.1 (re-test)	83.9 ± 3.0	65.7 ± 6.7	59	17
3	88.3 ± 7.0	74.5 ± 5.3	50	13
3.1 (re-test)	83.9 ± 3.9	49.5 ± 1.6	49	13
4	90.5 ± 2.6	74.3 ± 1.7	80	23
5	94.9 ± 4.6	71.2 ± 4.2	76	16
6	101.7 ± 5.7	73.0 ± 4.5	70	13
7	84.9 ± 4.6	70.3 ± 6.5	63	15
8	77.3 ± 7.4	64.8 ± 2.9	57	12

Table 2

Group (n = 6) *Z* statistic and volume (mean ± SD) for the Visual (Vis) and default mode networks. Corresponding ΔR2* and rCBV values for the pre and post ferumoxytol group are also presented, see also Figure 2 A.

Series	Visual Z score	Visual Volume (mm^3)	DMN Z score	DMN Volume (mm^3)
Pre-	4.54 ± 0.73	195.0 ± 55.7	4.38 ± 0.25	179.0 ± 28.4
Post-	4 71 ± 1.07	142.9 ± 49.0	4.22 ± 0.21	237.7 ± 50.6
Post96	4.05 ± 0.72	177.9.4 ± 76 1	4.39 ± 0.67	181.1 ± 38.8
Series	DR2* 10^{-2}	rCBV Id^{-2}	DR2* 10^{-2}	rCBV 10^{-2}
Pre-	3.66 ± 0.70	1.76 ± 0.18	3.64 ± 0.80	1 76 ± 0.40
Post-	3.26 ± 0.66	1.60 ± 0.21	3.38 ± 0.71	1.62 ± 0.26

Table 3

Subjects' body weight (Kg), injected blood iron concentration (mg/Kg), estimated millimolar blood iron concentration, T2* relaxation times, pre and post ferumoxytol infusion within the cortex (6 slices) and T2* relaxation rate within the sagittal sinus. ΔR2* within the sagittal sinus could not be accurately measured from the multiecho images because the second echo signal (TE 8.9ms) was almost in the noise. Measured blood ΔR2* was very weakly and inversely correlated with estimated blood ion concentration (R^2 = 0.09) or cortical ΔR2* (R^2 = 0.14). In contrast, cortical ΔR2* was positivelycorrelated with estimated blood iron concentration (R^2 = 0.59), as expected.

Subject #	Weight (Kg)	Fe conc. (mg/Kg)	Estimated Blood Iron conc (inM)	T2*-pre (ms) Cortex	T2*-post (ms) Cortex	ΔR2*(ms^{-1}) Cortex	ΔR2*(ms^{-1}) Blood
1	77.6	6.6	1.74	51.7 ± 2.0	26.1 ± 1.6	0.019 ± 0.002	0.39 ± 0.02
2	31.7	6.2	1.73	52.6 ± 2.5	24.7 ± 2.5	0.022 ± 0.003	0.52 ± 0.12
3	95.3	5.4	1.59	50.7 ± 2.2	24.3 ± 2.6	0.022 ± 0.004	0.56 ± 0.12
4	64.0	6.0	2.43	52.0 ± 3 7	21.4 ± 1.9	0.028 ± 0.003	0.55 ± 0.14
5	72.6	7.0	2.22	47.7 ± 2.9	18.9 ± 2.1	0.032 ± 0.005	0.32 ± 0.11
6	52.6	9.7	2.59	51.2 ± 2.9	19.3 ± 2.0	0.033 ± 0.005	0.21 ± 0.03
7	58.0	6.8	2.41	52.0 ± 2 9	21.0 ± 1.9	0.029 ± 0.003	0.51 ± 0.05
8	61.2	8.3	2.39	54.5 ± 4 3	20.3 ± 1.8	0.031 ± 0.003	0.56 ± 0.05